312

Copy
RM E52H07

NACA

NACA RM E52H07

RESEARCH MEMORANDUM

PROCEDURE FOR CALCULATING TURBINE BLADE TEMPERATURES AND COMPARISON OF CALCULATED WITH OBSERVED VALUES FOR TWO STATIONARY AIR-COOLED BLADES

By W. Byron Brown, Henry O. Slone, and Hadley T. Richards

Lewis Flight Propulsion Laboratory
Cleveland, Ohio

NATIONAL ADVISORY COMMITTEE
FOR AERONAUTICS

WASHINGTON

September 29, 1952

NATIONAL ADVISORY COMMITTEE FOR AERONAUTICS

RESEARCH MEMORANDUM

PROCEDURE FOR CALCULATING TURBINE BLADE TEMPERATURES AND COMPARISON OF CALCULATED WITH OBSERVED VALUES FOR TWO STATIONARY AIR-COOLED BLADES

By W. Byron Brown, Henry O. Slone, and Hadley T. Richards

SUMMARY

The accurate prediction of local turbine blade temperatures is necessary for the design of cooled turbines. When current methods of predicting blade temperatures are applied to cooled turbine blades, discrepancies between calculated and measured temperatures in some blade leading and trailing sections result. In an effort to reduce these discrepancies and hence to improve blade-temperature predictions, an investigation was conducted for stationary turbine blades with 10 tubes and 13 fins forming the internal heat-transfer surfaces. Local blade temperatures were calculated using previously published NACA temperature-distribution equations and the most recent theories for determining heat-transfer coefficients, including for the first time the allowance for effects of variable wall temperature on gas-to-blade heat-transfer coefficients at the leading and trailing sections of turbine blades. The calculated temperatures were compared with measured temperatures.

Results indicate that calculated trailing-section temperatures can be greatly reduced and leading-section temperatures increased in blades which have an appreciable temperature gradient in these sections when gas-to-blade heat-transfer coefficients based on variable wall temperature rather than coefficients based on constant wall temperature are used in the temperature-distribution equations. Applications of gas-to-blade coefficients based on variable wall temperature and an average blade-to-coolant coefficient for the coolant passage nearest the trailing edge for the 10-tube and 13-fin blades resulted in probable errors for a point near the trailing edge of 6° and 4° F, respectively, for a 300° F gas temperature and of 36° and 30° F, respectively, for a 1000° F gas temperature. For a point near the leading edge, a similar procedure resulted in probable errors of 5° and 6° F, respectively, for a 300° F gas temperature and of 8° and 18° F, respectively, for a 1000° F gas temperature. In the blade midchord region, where variable-wall-temperature effects are negligible, maximum probable errors of 8° and 13° F for gas temperatures of 300° F and 1000° F were obtained for the two blades.

INTRODUCTION

A knowledge of cooled-blade temperatures for a turbine of known design and operating conditions is extremely important in the evaluation of cooled turbines. Reliably calculated blade temperatures enable the turbine designer to (1) determine accurately the required coolant flow necessary for the turbine design characteristics considered, (2) examine the thermal gradients in the blade, because large thermal gradients may cause the blade to fail, and (3) determine the strength characteristics of the turbine blade on the basis of stress-to-rupture data. Blade strength decreases rapidly as the blade temperature increases; thus an accurate calculation of blade temperatures is required. Also, experimental and reliably calculated blade temperatures afford a check on the blade fabrication techniques; that is, a comparison between experimental and calculated temperatures may indicate whether or not the thermal bond between the internal heat-transfer surfaces and the blade shell is satisfactory.

As early as 1945, equations for calculating blade temperature distributions were developed and published by the NACA. These investigations are summarized in references 1 and 2. Because the accuracy of the calculated temperatures depends primarily on the heat-transfer coefficients inserted into the equations, it is quite important that appropriate values for these be determinable.

For forced-convection blade-to-coolant heat-transfer coefficients, hereinafter called inside coefficients, pipe correlations agree with experimental correlations for air in a stationary cascade (reference 3) and heated liquids in a rotating cascade (reference 4).

The gas-to-blade heat-transfer coefficients, hereinafter called outside coefficients, offer a more complex problem because turbine blade shapes differ widely among themselves and from round tubes, so that a great variety of pressure and velocity distributions occurs. For laminar flow, methods have been published for computing both average and local outside coefficients for a wedge-type flow which are applicable to turbine blades (reference 5). The conditions covered by that investigation for a constant wall temperature include an Euler number range (a measure of the pressure gradient) from -0.09 to 2.0, Mach numbers approximating zero, a Prandtl number range from 0.6 to 1.0, and a temperature ratio (gas to wall) equal to 1.0. Additional analyses of the laminar region which can also be applied to cooled blades with impermeable walls were made for the case of transpiration cooling. These analyses are presented in references 6 to 9.

An approximate method of solving the laminar-boundary-layer equations for cylinders of arbitrary cross section is presented in reference 6. This method requires that the velocity and temperature profiles

in the boundary layer be assumed. The conditions covered by this analysis include a constant wall temperature, a temperature ratio equal to 1.0, and a range of Prandtl number. An exact method of solving the laminar-boundary-layer equations for a wedge-type flow presented in reference 7 includes the conditions of a constant wall temperature, Euler number range from separation values to 1.0, Mach numbers approximating zero, a Prandtl number of 0.7, and temperature ratios from 1.0 to 4.0. Reference 8 presents a tabulation of these exact solutions of the laminar-boundary-layer equations for most of the conditions of reference 7 and includes results from two additional temperature ratios of 1/4 and 1/2. Another approximate method which utilizes prepared charts to reduce calculation procedures is presented in reference 9 for the calculation of heat transfer in the laminar region around cylinders of arbitrary cross section. This method is based on the exact boundary-layer solutions for wedge-type flow presented in references 7 and 8. The boundary-layer equations for cylinders of arbitrary cross section were used in reference 9 to compare the solutions obtained in references 7 and 8 for wedge-type flow. For impermeable blade walls, it can be shown (reference 9) that the effect of temperature ratios from 1.0 to 2.0 on heat transfer is negligible in the laminar region. At present, a temperature ratio of 2.0 is probably the limit for air-cooled blades having impermeable walls. Also, it is pointed out in reference 9 that heat-transfer coefficients obtained for elliptical cylinders compared favorably with those determined from wedge-type-flow solutions. On the basis of the foregoing results, the simplified methods reported in reference 5 for the determination of heat-transfer coefficients in the laminar region are currently adequate for application to air-cooled turbine blades having impermeable walls.

Local and average heat-transfer coefficients for turbulent flow are computed in references 5, 10, and 11 for the cases of zero pressure gradient (flat plate), constant wall temperature, low subsonic Mach numbers, temperature ratio equal to 1.0, and a Prandtl number range from 0.5 to 10.

An equation for the average outside heat-transfer coefficient for turbine blades including both laminar and turbulent flow is derived in reference 5 for constant wall temperature, low subsonic Mach numbers, temperature ratio equal to 1.0, and including the Euler number and laminar to turbulent transition-ratio effects. Calculated average outside coefficients using the equations of reference 5 compared favorably with observed data for stationary blades in references 12 and 13 and with data for a water-cooled turbine in reference 14.

The temperature equations reported in references 1 and 2 have been used recently to compute cooled-blade temperatures in stationary and rotating turbine blade cascades in which temperatures were measured experimentally. Reference 15 gives a comparison between calculated and

experimental blade temperatures for two stationary air-cooled blade configurations. One of the configurations investigated was a hollow aluminum blade with long leading and trailing sections. The other configuration was an air-cooled blade of low thermal conductivity with a long trailing section, a short leading section, and 10 tubes forming the internal heat-transfer surfaces. Hereinafter, the terms long leading and trailing sections will be used when referring to blades having a sufficiently large area of low thermal conductivity metal in the uncooled section to cause an appreciable temperature gradient. The methods reported in reference 5 were used to compute constant wall temperature outside coefficients for the calculations of reference 15; a stagnation point coefficient was used to calculate local leading section temperatures, and average outside coefficients were employed to calculate an average midchord and local trailing section temperatures. Good agreement was obtained for both blades at low and high gas temperatures except at the trailing section of the 10-tube blade where the calculated temperature was at least 100° F higher than the experimental value at a gas temperature of 1000° F.

A rotating cascade of air-cooled thin-shelled blades (blades having a mean wall thickness of approximately 0.040 in.) was used for a comparison of average calculated and experimental blade temperatures in reference 16. An average constant-wall-temperature outside coefficient was computed from reference 5 for the entire blade periphery, and the average calculated blade temperature was found to be approximately 30° F less than the experimental value for a gas temperature of approximately 1500° F. Reference 17 contains a comparison of calculated and experimental blade temperatures for the leading and trailing sections and the midchord region of an aluminum water-cooled turbine. Once again, the outside coefficients for constant wall temperature as computed from reference 5 were used in these calculations. Generally, good agreement resulted except at the leading section, where the maximum deviation was 47° F for a gas temperature range from 400° to 1600° F.

On the basis of the foregoing results, the methods reported in references 15 to 17 are considered accurate enough for calculating cooled-blade temperatures at the midchord region of most blades and at the leading and trailing sections of thin-shelled air-cooled blades. Also, reliable temperatures can probably be calculated for blades of high thermal conductivity even if the leading and trailing sections are physically long. The methods are not accurate enough for long leading and trailing sections of low thermal conductivity as indicated by the results described for the trailing section of the 10-tube air-cooled blade (reference 15). In future cooled-turbine-blade applications, liquid-cooled blades and possibly some cast air-cooled blades may be made of steel (low thermal conductivity) and have long leading and trailing sections. Since low conductivity in a long blade section is

conducive to appreciable temperature gradients in that section, a method of calculating blade temperatures more accurate than methods obtainable to date is desired.

As was pointed out in the preceding discussion, local trailing-section temperatures for a blade of low thermal conductivity and a long trailing section resulted in calculated temperatures at least 100° F higher than the experimental values. Such trends were noticed as long ago as 1943 by E. Schmidt (reference 18) who observed a much lower trailing-section temperature than he calculated. This result was attributed by E. R. G. Eckert to the shielding effect of the boundary layer, which is strongly cooled in the forward portion of the blade; that is, the metal temperature increases quite rapidly from the cooled midchord region to the edge of the long trailing section, especially where metals of low thermal conductivity are used. At the time, no method was given for evaluating this effect numerically. Recently, however, some attempts have been made to include these effects by consideration of variations in wall temperature on outside coefficients. References 19 to 21 consider laminar flow along flat plates and wedges, and reference 22 considers the case for turbulent flow of an incompressible fluid along a flat plate. Constant property values and pressure gradient effects are included in references 19 and 21, whereas reference 20 allows for certain variations in property values but does not include any pressure gradient effect. On the basis of the results of references 19 to 22, it can be concluded that the calculated trailing-section temperatures of the 10-tube blade (reference 15), which were considerably higher than the experimental values, may be partially attributed to the effects of an appreciable temperature gradient in the long trailing section.

Consequently, an investigation was conducted at the NACA Lewis laboratory on two air-cooled turbine blade configurations (the 10-tube blade of reference 15 and a 13-fin blade which has long leading and trailing sections) in order to (1) obtain local experimental blade temperatures around the blade periphery for two gas temperatures and a range of cooling-air flow, and (2) compare the data with calculated blade temperatures, wherein an attempt was made to eliminate the outstanding discrepancies obtained in previous investigations. The experimental investigation was conducted in a static cascade because the instrumentation could be more complete and accurate than on a rotating cascade.

The purposes of this report are to (1) apply variable-wall-temperature corrections to the outside coefficients for sections of the blade which require such corrections, and use these corrected coefficients to calculate blade temperatures, (2) compare the calculated temperatures with experimental temperatures obtained in the investigation just described in order to determine the adequacy of the variable-wall-temperature correction in reducing the differences between experimental

and calculated temperatures for long leading and trailing sections, and (3) present a detailed method for calculating local cooled-blade temperatures by use of the best available theories for obtaining outside and inside coefficients. The method of calculation is of such nature that it can be carried out entirely from design data without any test measurements.

The results of this investigation are presented for gas temperatures of 300° and 1000° F, a range of gas Mach number from 0.4 to 0.6, a mean temperature ratio (gas to average wall) of 1.40, a range of cooling-air flow for Reynolds numbers from 5000 to 40,000 for each gas temperature, and a range of Euler number in the laminar region from 1.0 to 0.

APPARATUS AND PROCEDURE

Test Facility

A sectional view of the blade test section used in this investigation is shown in figure 1. Combustion air passed successively through a flat-plate orifice, a combustor, and a plenum chamber prior to entering the test section, and then into the exhaust system. The gasoline combustor used in these investigations limited the gas temperature range to between 300° and 1000° F. The inlet duct to the test section was equipped with a bellmouth to insure a uniform velocity profile at the entrance to the cascade. The setup was insulated against heat loss from just downstream of the combustor to just downstream of the test section.

A cascade of seven blades was installed in the test section according to the dimensions in figure 2. The test blade, installed as the center blade, was the only blade through which cooling air was passed. The other six blades had the same profile as the test blade. The cooling air that was supplied to the test blade was obtained from the laboratory refrigerated air system. The air passed successively through a plenum chamber, the blade entrance extension, the test blade, the blade exit extension, another plenum chamber, a flat-plate orifice, and then into the laboratory exhaust system (see fig. 1). Because it was impossible to connect the plenum chambers directly to the blade, blade entrance and exit extensions of the same shape as the blades were used to conduct the air from the entrance plenum chamber to the test blade and from the test blade to the exit plenum chamber. The blade entrance extension had a span of 6 inches and the blade exit extension, a span of 3 inches. Both extensions had an internal free-flow area of 0.043 square inch and a hydraulic diameter of 0.396 inch. In order to reduce the amount of heat conducted from the ends of the hot test blade, metal was removed in the form of 1/8 inch wide chordwise slots cut through the walls of these extensions near the ends adjacent to the test blade. These slots were then sealed with a low conductivity material to prevent coolant leakage.

Blade Description

The air-cooled turbine blade configurations used in this investigation were a 10-tube blade and a 13-fin blade. The reason for selecting these two blade configurations is that the 13-fin blade has both long leading and trailing sections and the 10-tube blade has a long trailing section but a thin-shell leading section. Figure 3 shows the end views of the two blades. The geometry factors pertinent to the two blade configurations are given in the following table:

Geometry factor	10-tube blade	13-fin blade
Blade chord, in.	2.00	2.00
Outside perimeter, in.	4.35	4.53
Span, in.	3.92	3.50
Portion of blade span exposed to gas stream, in.	3.00	3.00
Total free-flow area of internal cooling-air passage, sq in.	.181	.0962
Hydraulic diameter of internal cooling-air passage, in.	.103	.0670

10-tube blade. - The 10-tube blade used in this investigation was similar to the 10-tube blades used in the investigations reported in references 15 and 23. The outside wall of the blade tapered linearly from the root to the tip for reduction of stresses during engine operation. The nominal thickness of the wall at the tip was 0.040 inch and at the base, 0.070 inch. The blade shell was cast of high-temperature alloy (X-40) in such a manner that the core area was constant over the length of the blade. In order to increase the internal heat-transfer surface, 10 tubes were inserted in the hollow blade (fig. 3). They extended through the blade from tip to base. These tubes were brazed to each other and to the inside surface of the hollow blade by Nicrobraze. Of the 10 tubes, four were made of stainless-steel tubing having a 0.125 inch outside diameter and a wall thickness of 0.010 inch; and six were made of low-carbon steel with a 0.156 inch outside diameter and a wall thickness of 0.0155 inch. Availability at the time of fabrication accounted for the difference in tubing materials.

13-fin blade. - The 13-fin blade used in this investigation was designed for heat-transfer investigations in a static cascade; therefore there was no taper in the blade wall, but the outside blade profile was essentially the same as for the 10-tube blade. The blade was machined in two parts divided essentially at the mean camber line, and upon assembly the parts were welded together at the leading and trailing edges; therefore the 13 fins were not continuous (see fig. 3). The fins had an average thickness of 0.036 inch, and the average fin spacing was 0.046 inch. The blade was machined from high-temperature alloy S-816.

Instrumentation

In order to calculate blade temperatures for the conditions of cascade operation, it was necessary that the cooling-air weight flow, the blade entrance cooling-air temperature, and the gas temperature be known. Also, for purposes of comparison, blade temperatures were measured for a range of cooling-air weight flows.

The cooling-air weight flow was measured by means of a flat-plate orifice downstream of the test section, and the cooling-air temperatures were measured by means of thermocouples in the entrance and exit plenum chambers (fig. 1). The exit cooling-air temperature was measured to check the calculated values of this temperature. The total temperature of the combustion gas was measured by means of thermocouples upstream of the test section, and the combustion-gas weight flow was measured by means of a flat-plate orifice upstream of the test section. The blade temperature distribution was measured by 11 thermocouples in the blade wall around the blade perimeter at the midspan (see fig. 3).

In order to obtain the cooling-air total temperatures at the blade entrance and exit, thermocouples were placed in the walls of the blade extensions to correct the values of cooling-air total temperatures measured in the plenum chambers for any heat picked up in the blade entrance and exit extensions. The method of correcting the cooling-air temperatures for the heat picked up in the blade entrance and exit extensions is reported in reference 24.

Cascade Operation

Blade temperatures were measured for the 10-tube and 13-fin blades for the following conditions:

Blade	Gas temperature (°F)	Gas Prandtl number	Gas Mach number	Gas weight flow ($\frac{lb}{sec}$)	Mean temperature ratio (gas to average wall)	Euler number, laminar region	Cooling-air weight flow per blade ($\frac{lb}{sec}$)	Cooling-air Reynolds number	Average blade inlet cooling-air temperature (°F)
10-tube	300 and 1000	0.672 and 0.654	0.40 to 0.60	3.5 to 4.5	1.32 and 1.61	1.0 to 0	0.010 to 0.070	5000 to 40,000	-50
13-fin	300 and 1000	0.672 and 0.654	0.40 to 0.60	5.0 to 6.0	1.28 and 1.38	1.0 to 0	0.005 to 0.022	5000 to 17,000	8

After the cooling-air weight flow was set, frequent checks were made on the blade temperatures in order to ascertain when steady-state conditions were reached. When the blade temperatures and the combustion-gas weight flow remained steady for approximately 15 minutes, the necessary readings were taken.

METHODS OF CALCULATION

The present investigation was limited for simplicity to one-dimensional blade temperature-distribution equations. In the central portion of the blade section, where the blade temperatures at different stations along the blade periphery do not differ very much, average values of chordwise blade temperatures were calculated for the entire region. At the two extreme sections, near the leading and trailing edges, large temperature gradients occurred between the surface swept by the coolant and the surface swept by the hot gas at a given spanwise distance from the blade root. Here, chordwise temperature distributions were calculated under the assumption that the heat conducted from the section in the spanwise direction was negligible when compared with that conducted chordwise from the outer blade surface to the coolant.

Blade temperatures were calculated from a design basis; that is, it was assumed that only the blade geometry, effective gas temperature, cooling-air weight flow, combustion-gas weight flow, blade velocity distribution, and blade entrance effective cooling-air temperature were known. The effective gas temperature was obtained from the definition of recovery coefficient, which is a function of the total, static, and effective gas temperatures. From the measured total gas temperature and the calculated velocity distribution, the static gas temperature was determined and used to calculate the effective gas temperature by assuming a recovery coefficient of 0.89 (reference 25). Inasmuch as the calculated temperature distributions are for the blade midspan position so that a comparison could be made between calculated and experimental blade temperatures, an average effective cooling-air temperature is required in the temperature-distribution equations. It is sufficiently accurate, because of the linear distribution of the cooling-air temperature, to use an arithmetic average of the cooling-air total temperatures at the blade entrance and blade exit for the average effective cooling-air temperature. Since the blade entrance cooling-air total temperature was known, the blade exit cooling-air temperature was calculated from the equations presented in reference 26.

For simplicity in presentation, the temperature-distribution equations required in this investigation and the methods for determining the outside and inside heat-transfer coefficients will be considered separately in the following sections.

Midchord-Blade-Temperature Equation

Average blade temperatures for the midchord section of the blade (see fig. 3) were obtained from equation (22) reported in reference 2. This equation, in the notation of this report, is

$$\frac{T_{g,e} - \overline{T}_B}{T_{g,e} - \overline{T}''_a} = \frac{1}{1+\lambda} \tag{1}$$

where

$$\lambda = \frac{\overline{h}_o \, l_o}{\overline{h}_f \, l_i} \tag{2}$$

(All symbols are defined in the appendix.) Blade temperatures were determined by inserting into the equations the appropriate perimeters of the blades in question and heat-transfer coefficients determined by methods to be discussed in subsequent sections of this report. The methods for determining $T_{g,e}$ and $\overline{T}''_a$ which are required in equation (2) have been discussed in the preceding section.

Chordwise-Temperature-Distribution Equation Through Blade Leading and Trailing Sections

The leading and trailing sections of the 10-tube and 13-fin blades were approximated by trapezoids. The one-dimensional blade chordwise-temperature-distribution equation for a trapezoidal approximation to the blade leading- and trailing-edge sections (equation (20), reference 1) is, in the notation of this report,

$$\frac{T_{g,e} - T^*_B}{T_{g,e} - \overline{T}''_a} = \frac{\dfrac{\overline{h}_i \, \zeta_2}{2K^2 \, k_B}\left[H_1(i\zeta_1)\, J_o(i\zeta) + iJ_1(i\zeta_1) iH_o(i\zeta)\right]}{\left[iJ_1(i\zeta_1)\, H_1(i\zeta_2)\right] - \left[H_1(i\zeta_1) iJ_1(i\zeta)_2\right] + \dfrac{\overline{h}_i \, \zeta_2}{2K^2 \, k_B}\Gamma} \tag{3}$$

The geometry factors and the effect of variable wall temperature on outside heat-transfer coefficients incorporated in the terms K, ζ, ζ_1, and ζ_2 were evaluated from their definitions given in reference 1 for a wedge approximation of the blade leading and trailing sections.

The temperature distributions in the leading and trailing sections were calculated by insertion of appropriate blade dimensions and by use of heat-transfer coefficients determined by the following methods.

Outside Heat-Transfer Coefficients

The use of different equations for the calculation of blade temperatures in various parts of an air-cooled turbine blade is accompanied by the use of different outside heat-transfer coefficients in these equations. Consequently, outside coefficients will be discussed for the midchord region, the trailing section, and the leading section in that order.

Midchord region of blade. - The following procedure was used to determine an average outside coefficient for the blade midchord region (fig. 3 shows blade midchord region). Local outside coefficients at three points near the beginning, middle, and end of the pressure surface of the blade midchord region and local coefficients at three similar points on the suction surface were computed. The equation (equation (19), reference 5)

$$Nu_g/Pr_g^{\frac{1}{3}} = \overline{F}_{lam}\sqrt{Re_g} \quad \text{(laminar flow)} \tag{4}$$

was used to calculate the local coefficients in the laminar region because, as pointed out in the INTRODUCTION, the simplified procedure of reference 5 is currently adequate for application to air-cooled impermeable-wall blades. For the calculation of local coefficients in the turbulent region, it is assumed that the effect of temperature ratios from 1.0 to 2.0 on heat-transfer coefficients is negligible, as was the case in the laminar region (reference 9). Consequently, the equation (equation (26), reference 5)

$$Nu_g/Pr_g^{\frac{1}{3}} = 0.0296\ Re_g^{0.8} \quad \text{(turbulent flow)} \tag{5}$$

was used to calculate the local coefficients in the turbulent region. An arithmetic average of the six local coefficients was used for the average outside coefficient for the blade midchord region. The fluid properties of equations (4) and (5) are based on an assumed wall temperature. Therefore, the calculation of an average blade midchord temperature is essentially an iteration process - an average blade midchord temperature is assumed to calculate an average outside coefficient, this coefficient is used in equation (1) to calculate an average blade midchord

temperature, and then the two values are compared. It can be shown from equation (1) that a 25 percent change in the assumed blade temperature will result in a change of approximately 3 percent in the calculated blade temperature.

The location of the transition point on each blade surface is required in order to determine whether laminar or turbulent flow prevails at each of the six local midchord points in question, and hence whether equation (4) or equation (5) is applicable at each of these points. Moreover, if equation (4) is applicable, a knowledge of the local Euler number is necessary for the calculation of $\overline{F}_{lam}$. The value of the local velocity, the location of the transition point (considered herein as the minimum pressure point), and the calculation of the required local Euler number

$$Eu = -(dp_g/dx)/(p_{g,\infty}U_{g,\infty}^2/x) \tag{6}$$

were all determined from the velocity distribution about the blade in question; the velocity distribution was calculated by the method of reference 12 and checked by measurements made on a Lucite blade of similar shape. From this calculated velocity distribution, the pressure distribution and hence the density were obtained. The Reynolds number, with properties based on wall temperature, was then determined.

Trailing section of blade. - The trailing sections of the blades considered in this investigation were approximated by trapezoids, to which equation (3) is applicable. In these blades, which have a long trailing section and are made of a high-temperature alloy (low thermal conductivity), the wall temperature varied rapidly beyond the coolant passage, and according to reference 22 the outside heat-transfer coefficient could consequently be quite different from the coefficients for a constant wall temperature. This difference was provided for by use of a curve for the turbulent boundary layer (fig. 4) which is based on approximate analytical results of reference 22. The analysis of reference 22 is subject to the assumptions of a flat plate (no pressure gradient), constant property values, and no frictional dissipation of energy within the boundary layer. Since it can be assumed that trailing sections of turbine blades have a negligible pressure gradient and the effects of the other two assumptions are quite small, figure 4 should be applicable for trailing sections of turbine blades which have an appreciable temperature gradient. Figure 4 presents the ratio of the outside heat-transfer coefficient for variable wall temperature to that for constant wall temperature as a function of the exponent n, where n is given by the relation

$$\frac{T_{g,e} - T_B^*}{T_{g,e} - T_B} \approx X^n \tag{7}$$

and X is measured along the profile from a reference point where the midchord region with uniform temperature T_B ends and the region of rapid change in wall temperature T_B^* begins. In the investigations reported herein, this reference point was taken at the end of the tube or fin section (see fig. 3).

Equation (67) of reference 22, derived for a flat plate and turbulent flow, expresses the relation between the heat-transfer coefficients based on variable and constant wall temperatures. In the notation employed herein, equation (67) is

$$\frac{h_o^*}{\bar{h}_{o,X}} = \frac{\sum_n A_n Y_n (X/j)^n}{\sum_n A_n (X/j)^n} \tag{8}$$

where $\sum_n A_n (X/j)^n$ is a power series expansion of the temperature ratio $\left[(T_{B,X}/T_{g,\infty})-1\right]$ and Y_n is a relation among certain gamma functions defined as

$$Y_n = \frac{\Gamma\left(\frac{40n}{39}+1\right)\Gamma\left(\frac{32}{39}\right)}{\Gamma\left(\frac{40n}{39}+\frac{32}{39}\right)} \tag{9}$$

In the calculations necessary for the construction of figure 4, only one term in the series expansion was considered so that equation (8) simplified to

$$\frac{h_o^*}{\bar{h}_o} = Y_n \tag{10}$$

Values of n were inserted into equation (9) to obtain a set of ratios of the variable- to constant-wall-temperature heat-transfer coefficients.

When an attempt is made to apply figure 4 to calculations for a blade trailing section, the value of n is unknown. However, a value of h_o (constant-wall-temperature outside coefficient) can be determined by the method employed in calculating the midchord coefficient. In this instance, two local outside coefficients were calculated on each surface of the trailing section by application of equation (5) (turbulent flow prevails over the blade trailing section). The average of these four local coefficients $\bar{h}_o$ was used along with an assumed value of n, say -0.6, and $\bar{h}_o^*$ (variable-wall-temperature average outside coefficient) was then obtained by use of figure 4. The temperature distribution was then calculated by use of equation (3). Since the

value of $T_{g,e}$ was known, a logarithmic plot of $T_{g,e} - T_B^*$ against X determined n. If this value equaled the assumed n, the temperature distribution was the required one; if the two values of n differed, n was adjusted until the initial and final values agreed, and the desired value of $\overline{h}_o^*$ was obtained from figure 4.

Leading section of blade. - The effect of variable wall temperature on outside heat-transfer coefficient was also taken into consideration for the blade leading section. Here laminar flow prevails, and the analysis of reference 21 for wedge flows, flat-plate flow, and stagnation flow, assuming constant property values, was used to account for the effect of variable wall temperature. Figure 5 gives the relation between the outside heat-transfer coefficients for variable and constant wall temperatures as a function of the exponent n (see equation (7) wherein X is replaced by x for this case). The values used in constructing figure 5 were obtained from table 1 (Euler number of zero) and table 2 (Euler number of 1.0) of reference 21 for a Prandtl number of 0.7 by dividing the outside coefficients for various values of n (variable wall temperature) by the value for n equal to zero (constant wall temperature). Since the leading sections of turbine blades are in the laminar region and have Euler numbers ranging from 1.0 (stagnation point) to zero (transition from laminar to turbulent), figure 5 is applicable to blade leading sections. For this investigation, the constant-wall-temperature outside coefficient was determined in a way similar to that for the midchord coefficient, that is, as an average of 12 local outside coefficients (six on each blade surface located between the coolant passage nearest the blade leading section and the stagnation point) determined from equation (4) for constant property values. Also, local Euler numbers were calculated for the 12 points and averaged. Therefore, figure 5 and values of $\overline{h}_o$ and $\overline{Eu}$ were used to determine $\overline{h}_o^*$ for the leading section in the manner used for the trailing-section turbulent-flow outside coefficient. For the leading section, however, x was measured from the stagnation point, as in reference 21.

2630

Inside Heat-Transfer Coefficient

Different inside heat-transfer coefficients were required for use in the two temperature-distribution equations (equations (1) and (3)). In the midchord region of the blades, the heat-transfer surface area was greatly augmented by the use of tubes and fins. In order to make allowance for this, a so-called effective inside coefficient was required. On the other hand, heat leaving either the leading or trailing blade section is picked up by the cooling air adjacent to each section, and the presence of tubes or fins in the midchord region had little or no effect. Consequently, an average inside coefficient for the coolant which swept the leading and trailing sections was required for

the calculation of temperatures in these regions. The methods of determining the effective and the average blade-to-coolant heat-transfer coefficients that were required follow.

Effective coefficient. - For the midchord region of the blades, where the tubes or fins substantially increased the heat-transfer surface area, an effective coefficient was determined. An average heat-transfer coefficient for fully developed turbulent flow in pipes was obtained from equation (90) of appendix F, reference 26,

$$Nu_a = 0.019\ Re_a^{0.8} \tag{11}$$

The fluid property values in equation (11) were based on wall temperature in references 16 and 26, which was considered adequate for these investigations. It can be shown (reference 27) that for air flowing in a smooth round tube, a satisfactory correlation of average inside heat-transfer coefficients was obtained for a range of wall temperatures from approximately 150° to 1600° F and an inlet-air temperature near 75° F when the fluid properties were based on wall temperatures. When the range of wall temperatures was extended to cover a more complete range from approximately 75° to 2600° F and the inlet-air temperature varied from 75° to 1000° F, a good correlation of the heat-transfer data was obtained only when the fluid properties were based on film temperature (an average of the air and wall temperatures); it was assumed in reference 27 that the thermal conductivity of the air varied as the square root of the temperature. Since the best correlation of heat-transfer data over an extended range of wall temperature and inlet-air temperature was obtained when the fluid properties were based on film temperature, the fluid property values in equation (11) were based on film temperature (an average of the cooling-air and wall temperatures) in this investigation.

The required effective inside coefficient, based on inner wall surface area only, was determined from equation (6) of reference 16, which in the notation employed herein is

$$\bar{h}_r = \frac{\bar{h}_i}{\sum_{r=1}^{s} \alpha_r (m_r + \tau_r)} \left[\sum_{r=1}^{s} \frac{\alpha_r (2L_r) \tanh (L_r \varphi_r)}{L_r \varphi_r} + \sum_{r=1}^{s} \alpha_r m_r \right] \tag{12}$$

where $\bar{h}_i$ is obtained from equation (11) and is based on film temperature.

For application to air-cooled turbine blades with internal surfaces other than fins, the 10-tube blade in this instance required replacement of the internal surface by equivalent fins. The following general method of reference 16 was used:

(1) By inspection, the blade was divided into s sections of equivalent fins which appeared to have equal fin lengths, spacings, and thicknesses, and the number of fins α_r in each section was determined.

(2) For each section, the inside blade shell perimeter $l_{i,r}$ $\left[l_{i,r} = \alpha_r (m_r + \tau_r)\right]$ and the total wetted perimeter $l_{i,W,r}$ were determined.

(3) The quantities required for equation (12) were determined by the following definitions:

$$\alpha_r m_r = l_{i,r} - \alpha_r \tau_r \tag{13}$$

and

$$L_r = \frac{l_{i,W,r} - \alpha_r m_r}{2\alpha_r} \tag{14}$$

The relation between $\bar{h}_f$ and $\bar{h}_i$ for the 10-tube and 13-fin blades is shown in figure 6. Examples showing the application of equation (12) to tube- and fin-type blades are presented in appendix B of reference 16.

Average coefficient. - Average inside coefficients for computing leading- and trailing-section temperatures were calculated from equation (11). In each case, the coefficient was determined for the coolant which swept the one end of the blade section in question, and the dimensions of this particular passage were used in equation (11). The coolant flow for each of these passages was taken as the average coolant flow per unit of flow area.

Since $\bar{h}_i$ required for both leading- and trailing-section temperature calculations and for determining $\bar{h}_f$ is based on film temperature, which necessitates the assumption of a wall temperature, an iterative process similar to that used in calculating midchord outside coefficients was used here.

RESULTS AND DISCUSSION

The comparisons of calculated and measured blade temperatures for the 10-tube and 13-fin blades for the conditions of this investigation (listed previously in APPARATUS AND PROCEDURE section) are shown in figures 7 to 9 for the midchord, trailing, and leading sections of the blades, respectively. In each case the calculated temperatures are plotted as the ordinates and the measured temperatures, as the abscissas, with the 45° line representing perfect agreement.

Comparison of Calculated and Measured Midchord Blade Temperatures

Calculated midchord temperatures are compared with measured midchord temperatures in figure 7. In this region, temperatures were observed on each of the blade surfaces and the arithmetic average of these measurements was used to represent the measured midchord temperature. For the calculation of the midchord temperatures, the average effective inside heat-transfer coefficient was obtained by considering three groups of fins (or effective fins) for each of the blades. It must be remembered that in some cases more fin groups might be necessary since it is not advisable to average fins (or tubes) which differ very much in dimensions.

Figure 7 shows that the calculated and measured midchord temperatures agree very closely for both the 10-tube and 13-fin blades; that is, the points for both blades are very close to the 45° perfect agreement line. The quantity usually selected to compare the magnitudes of errors is the probable error (the number of errors greater than the probable error is the same as the number less than the probable error). For the midchord temperatures of the blades investigated, the probable error was found to be a maximum of 8° F for a gas temperature of 300° F and a maximum of 13° F for the 1000° F gas temperature. The good agreement between calculated and experimental temperatures clearly shows that departures from Mach numbers close to zero and a temperature ratio of 1.0 (the conditions used in obtaining equations (4) and (5)) are not enough to require corrections in the present investigation. Also, the assumption that the effect of temperature ratios from 1.0 to 2.0 on heat-transfer coefficients in the turbulent region is negligible appears to be justified. The applicability of equations (4) and (5) to other blade configurations and conditions will be discussed in a subsequent section of this report.

Comparison of Calculated and Measured Temperatures

Near Blade Trailing Edge

In figure 8, calculated blade temperatures are plotted against measured temperatures for the thermocouple located nearest the trailing edge of each blade (see fig. 3). For the 300° F gas temperature the agreement is again very good; the probable error for the 10-tube blade was found to be 6° F and for the 13-fin blade, 4° F.

For the 1000° F gas temperature, the probable errors were 36° F and 30° F for the 10-tube and 13-fin blades, respectively. Trailing-section temperatures were also calculated with no allowance for the effect of variation in wall temperature on the outside heat-transfer coefficient, and the calculated temperatures were at least 100° to 150° F higher than

the measured temperatures (see reference 15 for 10-tube blade results). It thus appears that outside heat-transfer coefficients which include wall-temperature-variation effects should be used in equation (3) for calculating accurate temperatures in cooled blades with long trailing sections.

The relatively large probable errors obtained for the trailing section of the blades at the 1000° F gas temperature may be due to separation of flow along this section of each blade. Calculated temperatures are dependent on the use of appropriate outside heat-transfer coefficients; since no method for the calculation of such coefficients is as yet known for separated regions, special corrections for separation of flow cannot be made at the present time - the separated region is simply included in the turbulent region. However, the conditions of equation (5) - negligible pressure gradient, low subsonic Mach numbers, and a temperature ratio equal to 1.0 - were fulfilled closely enough in the present investigation that the use of equation (5) precludes serious differences between experimental and calculated trailing-section temperatures. The justification of the assumption that the temperature ratio has a negligible effect on heat transfer in the turbulent region is not so apparent from these results as for the midchord temperature calculations.

Comparison of Calculated and Measured Temperatures

Near Blade Leading Edge

A plot of calculated against measured blade temperatures for the thermocouple located nearest the blade leading edge is shown in figure 9. Agreement at this point is also good. The maximum deviation between calculated and measured temperatures was found in the case of the 13-fin blade when the gas temperature was 1000° F. The probable errors were found to be 5° and 8° F for the 10-tube blade and 6° and 18° F for the 13-fin blade for gas temperatures of 300° and 1000° F, respectively.

Temperatures were also calculated for this blade location by use of outside coefficients based on constant wall temperature for the 1000° F gas temperature. Calculated temperatures were found to be of the order of 50° to 70° F below the measured values for the 13-fin blade, which has a long leading section. A negligible difference between calculated and measured temperatures for the 10-tube blade which has a short leading section (thin shell) resulted. Thus, in order to be able to calculate leading-section temperatures accurately, outside coefficients, which allow for variations in wall temperature, should be used in equation (3) for blades with long leading sections, whereas constant-wall-temperature outside coefficients may be used in equation (3) for blades with short leading sections (thin shell).

For the present investigation the fact that equation (4) and figure 5, used to determine the outside coefficients, are based on constant property values has little effect on the coefficients, because for the laminar region a change from constant property values results in a change of less than 1.0 percent in the coefficient (references 7 to 9).

Influence of Errors in Calculated Temperatures on Design Considerations

The agreement between calculated and measured temperatures at all locations on the blades investigated is considered to be well within the accuracy required for turbine design. Errors in prediction of blade temperatures in the trailing or leading sections are less serious than in the midchord region because evidence from endurance tests (reference 28) and calculations based on reference 29 indicate that the midchord region of the blade is the main stress carrying member. The effect of errors in calculated average blade midchord temperatures on blade material life will therefore be discussed.

At gas temperatures higher than the 1000° F temperature investigated herein, the probable errors in the calculated midchord temperatures would be somewhat higher. An increase in gas temperature from 300° to 1000° F resulted in an increase in the maximum probable error from 8° to 13° F for the midchord-temperature calculations. With stress-rupture characteristics as a basis, for most low-alloy steels suitable for nonstrategic turbine blades 25° F is about the maximum error permissible for design practice. For example, consider a turbine rotor blade made from Timken 17-22A(S) steel, centrifugally stressed to 25,000 pounds per square inch at the critical section, and designed for a stress-ratio factor of 2.0. (The stress-ratio factor is an indication of the blade stress carrying capacity and is defined in reference 29 as the ratio of the integrated allowable stress to the integrated centrifugal stress at the blade critical section.) An error of ±25° F in the average midchord temperature would result in stress-ratio factors of 2.36 and 1.56, respectively. On the basis of limited results, it is indicated in references 28 and 29 that turbine design calculations should be based on stress-ratio factors above 1.5. It is believed that for the higher gas temperatures encountered in current turbine engines, approximately 1700° F, the probable error in the calculated average midchord temperature would not exceed the permissible value of 25° F. Modifications to this calculation method for other blade configurations and conditions are given in the following section.

APPLICATION OF ANALYSIS TO OTHER BLADE CONFIGURATIONS AND CONDITIONS

The 10-tube and 13-fin blades were selected for this investigation because they had long leading and trailing sections (sufficient amount of low thermal conductivity metal area in section to cause an appreciable temperature gradient), except the leading section of the 10-tube blade, and large differences in coolant passage geometry. The results already presented indicate that calculated trailing-section temperatures are greatly reduced and leading-section temperatures increased in blades which have an appreciable temperature gradient in these sections when outside heat-transfer coefficients are corrected by newly published formulas for variable wall temperatures. Also, the results show that the same calculation procedures applied equally well to both blades and hence that passage configuration effects are negligible. However, the use of equation (1) yielded only an average midchord temperature at the blade midspan position. In order to calculate an average blade midchord temperature at a position other than midspan for a stationary blade, equation (20) of reference 2 must be applied. This equation requires that the effective cooling-air temperature at the blade root be known, whereas equation (1) of this investigation utilizes an average cooling-air temperature. For rotating blades, equation (18) of reference 2 is applicable; in this case, too, the blade root effective cooling-air temperature must be known. However, for calculating local temperatures at the leading and trailing sections, equation (3) is still applicable.

The procedure just described is applicable to other configurations with long leading and trailing sections (long metal heat-conduction paths). On the other hand, blades such as those reported in references 29 and 30 have thin blade shells so that the cooling-air passages are extended well into the leading and trailing sections and the wall-temperature variations in these regions are greatly reduced. For such blades the effect of wall-temperature variation can often be neglected and the calculation of blade temperatures is simplified by using the outside heat-transfer coefficients calculated by means of equations (4) and (5) without making a correction for wall-temperature variation. This was verified in the present investigation by the leading-section calculations for the 10-tube blade which has a thin-shell leading section. That is, the correction in the outside heat-transfer coefficient for the 10-tube blade leading section was only about 2 percent, whereas that for the 13-fin blade leading section was 20 percent. A comparison of calculated and measured average blade temperatures for two thin-shell blades investigated in a turbojet engine using the simplified method (no variable-wall-temperature correction) resulted in errors in calculated temperatures of about 30° F (reference 16). Some of this error may have been due to poor contact between the internal heat-transfer surface and the shell of the blades, although it may be possible that the theories verified in this investigation are not entirely adequate for rotating air-cooled blades.

For forced-convection liquid-cooled turbine blades with long leading and trailing sections, exactly the procedure described herein can be used to account for the variable-wall-temperature effect when calculating outside heat-transfer coefficients. The inside heat-transfer coefficient should be calculated by means of an appropriate pipe correlation, as shown in reference 4.

The effect of temperature ratio may in some cases be an important condition influencing outside heat-transfer coefficients. Nevertheless, the effect seems to be negligible for temperature ratios from 1.0 to 2.0. As pointed out earlier, a temperature ratio (gas-to-wall) of 2.0 is the probable limit for current air-cooled blades with impermeable walls. Also, even though turbine inlet temperatures may exceed 1700° F in the near future, it is believed that the temperature ratio will still be close to 2.0 for air-cooled blades with impermeable walls. Consequently, the methods employed in this investigation may be utilized for such high-temperature applications. For future cooled-turbine designs, probably those utilizing transpiration or liquid cooling, where temperature ratios higher than 2.0 may be encountered, the methods used herein must be modified. A detailed discussion of these modifications is beyond the scope of this report.

SUMMARY OF RESULTS

Temperatures calculated from previously published NACA equations and measured blade temperatures were compared for a 10-tube and a 13-fin air-cooled turbine blade tested in a static cascade. The results of this investigation for gas temperatures of 300° and 1000° F, subsonic gas Mach numbers, mean temperature ratios (gas-to-average wall) of 1.3 to 1.6, and a range of cooling-air weight flow are summarized as follows:

1. For those blades having long leading and trailing sections (sufficient amount of low thermal conductivity metal area in section to cause an appreciable temperature gradient), calculated trailing-section temperatures were greatly reduced and leading-section temperatures increased when outside heat-transfer coefficients were corrected by newly published formulas for variable wall temperatures.

2. For the midchord region of the blades investigated, the maximum probable error between calculated and measured blade temperatures was 8° F at a gas temperature of 300° and 13° F at a 1000° F gas temperature.

3. For the trailing section of the blade, the probable errors were 6° and 4° F at the 300° F gas temperature and 36° and 30° F at the 1000° F gas temperature for the 10-tube and 13-fin blades, respectively.

4. For the leading section of the blade, the probable errors were 5° and 6° F at the 300° F gas temperature and 8° and 18° F at the 1000° F gas temperature for the 10-tube and 13-fin blades, respectively.

5. The short (thin shell) leading section of the 10-tube blade required only a 2 percent correction of the outside heat-transfer coefficient for the variable-wall-temperature effect, whereas the long leading section of the 13-fin blade required a 20 percent correction.

Lewis Flight Propulsion Laboratory
National Advisory Committee for Aeronautics
Cleveland, Ohio

APPENDIX - SYMBOLS

The following symbols are used in this report:

A	flow area of coolant passage, sq ft
A_n	coefficients of power series
c_p	specific heat at constant pressure, Btu/(lb)(°F)
D_h	hydraulic diameter, $\frac{4 \text{ times flow area}}{\text{wetted perimeter}}$, ft
Eu	Euler number, $-(dp_g/dx)/(\rho_{g,\infty} U^2_{g,\infty}/x)$
$\overline{F}_{lam}$	variable, evaluated in figure 8, reference 5
h	local heat-transfer coefficient (constant wall temperature), Btu/(sec)(sq ft)(°F)
$\overline{h}$	average heat-transfer coefficient, Btu/(sec)(sq ft)(°F)
$\overline{h}_f$	average effective inside heat-transfer coefficient, Btu/(sec)(sq ft)(°F)
h_o^*	local outside heat-transfer coefficient (variable wall temperature), Btu/(sec)(sq ft)(°F)
$\overline{h}_o^*$	average outside heat-transfer coefficient (variable wall temperature), Btu/(sec)(sq ft)(°F)
iH_o, H_1	Bessel functions
j	chordwise distance from blade trailing or leading edge to coolant passage, ft
J_o, iJ_1	Bessel functions
K	$\left(\frac{\overline{h}_o^*}{k_B \sin \psi}\right)^{\frac{1}{2}}$
k	thermal conductivity, Btu/(sec)(ft)(°F)
L_r	fin length of fins in group r, ft (see equation (14))

l	perimeter, ft
m_r	spacing of fins in group r, ft
Nu_a	Nusselt number of cooling air, $(\bar{h}_i D_h)/k_{a,F}$
Nu_g	Nusselt number of gas, $h_o x/k_{g,w}$
n	exponent of X in relation $(T_{g,e} - T_B^*)/(T_{g,e} - T_B) \approx X^n$
Pr_g	Prandtl number of gas, $(c_{p,g,w}\mu_{g,w})/k_{g,w}$
p	static pressure, lb/sq ft absolute
Re_a	Reynolds number for cooling air, $(w_a D_h)/(A \mu_{a,F})$
Re_g	Reynolds number for gas, $(U_{g,\infty} \rho_{g,w} x)/\mu_{g,w}$
r	index of summation
s	number of fin groups
T	temperature, $^\circ F$
$\bar{T}$	average temperature, $^\circ F$
$\bar{T}_a''$	average cooling-air total temperature, $^\circ F$
T_B^*	blade temperature for case with variable wall temperature, $^\circ F$
U	velocity, ft/sec
w	air weight flow, lb/sec
X	distance along blade surface as shown in figure 3, ft
x	distance along blade surface from stagnation point, ft
Y_n	function defined by equation (8)
y	distance from blade trailing or leading edge to blade element, ft (see reference 1)
α_r	number of fins in group r

2630

Γ $H_1(i\zeta_1)\, J_0(i\zeta_2) + iJ_1(i\zeta_1)\, iH_0(i\zeta_2)$ except in equation (9), where Γ denotes the usual gamma function

ζ, ζ_1, ζ_2 $2K\left[y' + \frac{\tau_1(1 - \tan\psi)}{2\tan\psi}\right]^{\frac{1}{2}}$, $2K\left[\frac{\tau_1(1 - \tan\psi)}{2\tan\psi}\right]^{\frac{1}{2}}$, $2K\left[j' + \frac{\tau_1(1 - \tan\psi)}{2\tan\psi}\right]^{\frac{1}{2}}$

λ $\frac{\bar{h}_o l_o}{\bar{h}_f l_i}$

μ viscosity, lb/(ft)(sec)

ρ density, lb/(cu ft)

τ_1, τ_2 trapezoidal thicknesses at leading or trailing edge and coolant passage, respectively, ft

τ_r thickness of fins in group r, ft

φ_r $\left(\frac{2\,\bar{h}_i}{k_B\,\tau_r}\right)^{\frac{1}{2}}$ where $\bar{h}_i$ is based on film temperature

ψ $\tan^{-1}\left(\frac{\tau_2 - \tau_1}{2j}\right)$

Subscripts:

a air

B blade

e effective

F evaluated at film temperature

g gas

i inside

o outside

r any internal section of blade formed by fins or equivalent fins

W wetted

w evaluated at wall temperature

X local point

∞ free stream

Superscripts:

' denotes linear dimension increased by $\tau_1/2$

* refers to variable wall temperature

REFERENCES

1. Livingood, John N. B., and Brown, W. Byron: Analysis of Temperature Distribution in Liquid-Cooled Turbine Blades. NACA Rep. 1066, 1952. (Supersedes NACA TN 2321.)

2. Livingood, John N. B., and Brown, W. Byron: Analysis of Spanwise Temperature Distribution in Three Types of Air-Cooled Turbine Blade. NACA Rep. 994, 1950. (Supersedes NACA RM's E7B11e and E7G30.)

3. Cohen, H.: Heat Transfer in Air-Cooled Gas-Turbine Blades. Engineering, vol. 173, no. 4484, Jan. 4, 1952, pp. 21-23.

4. Freche, John C., and Schum, Eugene F.: Determination of Blade-to-Coolant Heat-Transfer Coefficients on a Forced-Convection, Water-Cooled, Single-Stage Turbine. NACA RM E51E18, 1951.

5. Brown, W. Byron, and Donoughe, Patrick L.: Extension of Boundary-Layer Heat-Transfer Theory to Cooled Turbine Blades. NACA RM E50F02, 1950.

6. Eckert, E. R. G., and Livingood, John N. B.: Calculations of Laminar Heat Transfer Around Cylinders of Arbitrary Cross Section and Transpiration-Cooled Walls with Application to Turbine Blade Cooling. NACA RM E51F22, 1951.

7. Brown, W. Byron: Exact Solution of the Laminar Boundary Layer Equations for a Porous Plate with Variable Fluid Properties and a Pressure Gradient in the Main Stream. Paper presented at First U.S. National Congress of Applied Mechanics (Chicago), June 11-16, 1951.

8. Brown, W. Byron, and Donoughe, Patrick L.: Tables of Exact Laminar-Boundary-Layer Solutions When the Wall is Porous and Fluid Properties are Variable. NACA TN 2479, 1951.

9. Eckert, E. R. G., and Livingood, John N. B.: Method for Calculation of Heat Transfer in Laminar Region of Air Flow Around Cylinders of Arbitrary Cross Section (Including Large Temperature Differences and Transpiration Cooling). NACA TN 2733, 1952.

10. Boelter, L. M. K., Grossman, L. M., Martinelli, R. C., and Morrin, E. H.: An Investigation of Aircraft Heaters. XXIX - Comparison of Several Methods of Calculating Heat Losses from Airfoils. NACA TN 1453, 1948.

11. Johnson, H. A., and Rubesin, M. W.: Aerodynamic Heating and Convective Heat Transfer - Summary of Literature Survey. Trans. A.S.M.E., vol. 71, no. 5, July 1949, pp. 447-456.

12. Hubbartt, James E., and Schum, Eugene F.: Average Outside-Surface Heat-Transfer Coefficients and Velocity Distributions for Heated and Cooled Impulse Turbine Blades in Static Cascades. NACA RM E50L20, 1951.

13. Donoughe, Patrick L.: Outside Heat Transfer of Bodies in Flow-A Comparison of Theory and Experiment. Thesis submitted to Case Inst. Tech., June 1951.

14. Freche, John C., and Schum, Eugene F.: Determination of Gas-to-Blade Convection Heat-Transfer Coefficients on a Forced-Convection, Water-Cooled Single-Stage Aluminum Turbine. NACA RM E50J23, 1951.

15. Ellerbrock, Herman H., Jr.: Some NACA Investigations of Heat-Transfer of Cooled Gas-Turbine Blades. Paper presented at the General Discussion on Heat Transfer. Inst. Mech. Eng. (London) and A.S.M.E. (New York) Conference (London), Sept. 11-13, 1951.

16. Ziemer, Robert R., and Slone, Henry O.: Analytical Procedures for Rapid Selection of Coolant Passage Configurations for Air-Cooled Turbine Rotor Blades and for Evaluation of Heat-Transfer, Strength, and Pressure-Loss Characteristics. NACA RM E52G18, 1952.

2630

17. Schum, Eugene F., Freche, John C., and Stelpflug, William J.: Comparison of Calculated and Experimental Temperatures of Water-Cooled Turbine Blades. NACA RM E52D21, 1952.

18. Petrick, E. N.: A Survey of German Hollow Turbine Blade Development. Pt. I - Initial Investigations and Developments. Purdue Univ., Purdue Res. Foundation, pub. by USAF-AMC, Wright-Patterson Air Force Base, Dayton (Ohio) Oct. 1949.

19. Schuh, H.: Laminar Heat Transfer in Boundary Layers at High Velocities. Rep. and Trans. 810, British M.A.P., April 15, 1947.

20. Chapman, Dean R., and Rubesin, Morris W.: Temperature and Velocity Profiles in the Compressible Laminar Boundary Layer with Arbitrary Distribution of Surface Temperature. Jour. Aero. Sci., vol. 16, no. 9, Sept. 1949, pp. 547-565.

21. Levy, Solomon: Heat Transfer to Constant-Property Laminar Boundary-Layer Flows with Power-Function Free-Stream Velocity and Wall-Temperature Variation. Jour. Aero. Sci., vol. 19, no. 5, May 1952, pp. 341-348.

22. Rubesin, Morris W.: The Effect of an Arbitrary Surface-Temperature Variation Along a Flat Plate on the Convective Heat Transfer in an Incompressible Turbulent Boundary Layer. NACA TN 2345, 1951.

23. Ellerbrock, Herman H. Jr., and Stepka, Francis S.: Experimental Investigation of Air-Cooled Turbine Blades in Turbojet Engine. I - Rotor Blades with 10 Tubes in Cooling-Air Passages. NACA RM E50I04, 1950.

24. Brown, W. Byron, and Slone, Henry O.: Pressure Drop in Coolant Passages of Two Air-Cooled Turbine-Blade Configurations. NACA RM E52D01, 1952.

25. Esgar, Jack B., and Lea, Alfred L.: Determination and Use of the Recovery Factor for Calculating the Effective Gas Temperature for Turbine Blades. NACA RM E51G10, 1951.

26. Brown, W. Byron, and Rossbach, Richard J.: Numerical Solution of Equations for One-Dimensional Gas Flow in Rotating Coolant Passages. NACA RM E50E04, 1950.

27. Humble, Leroy V., Lowdermilk, Warren H., and Desmon, Leland G.: Measurements of Heat-Transfer and Friction Coefficients for Subsonic Flow of Air in Smooth Tubes at High Surface and Fluid Temperatures. NACA Rep. 1020, 1951. (Supersedes NACA RM's E7L31, E8L03, E50E23 and E50H23.)

28. Stepka, Francis S., and Hickel, Robert O.: Experimental Investigation of Air-Cooled Turbine Blades in Turbojet Engine. IX - Evaluation of the Durability of Noncritical Rotor Blades in Engine Operation. NACA RM E51J10, 1951.

29. Esgar, Jack B., and Clure, John L.: Experimental Investigation of Air-Cooled Turbine Blades in Turbojet Engine. X - Endurance Evaluation of Several Tube-Filled Rotor Blades. NACA RM E52B13, 1952.

30. Bartoo, Edward R., and Clure, John L.: Experimental Investigation of Air-Cooled Turbine Blades in Turbojet Engine. XII - Cooling Effectiveness of a Blade with an Insert and with Fins Made of a Continuous Corrugated Sheet. NACA RM E52F24, 1952.

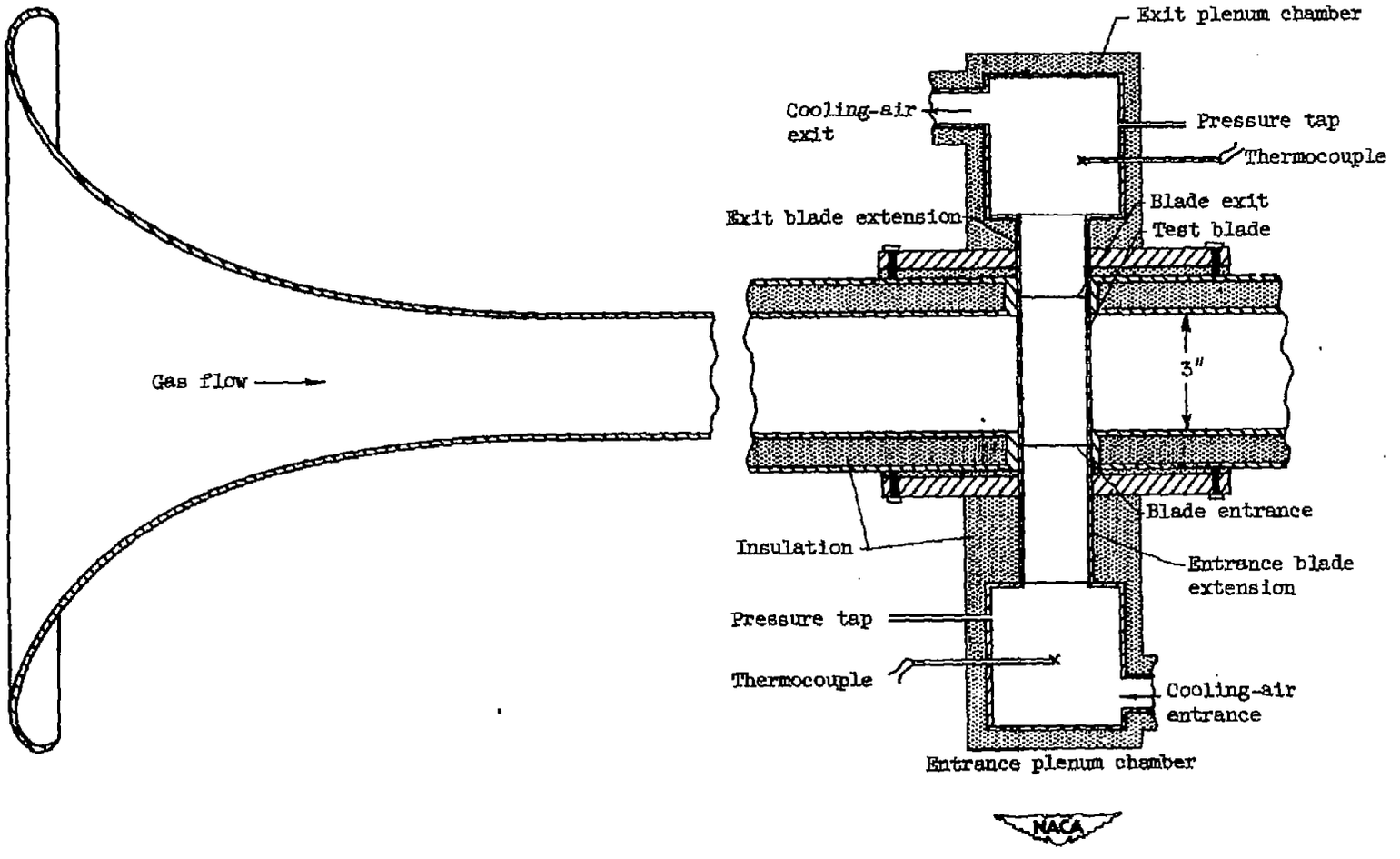

Figure 1. - Sectional view of blade test section showing instrumentation.

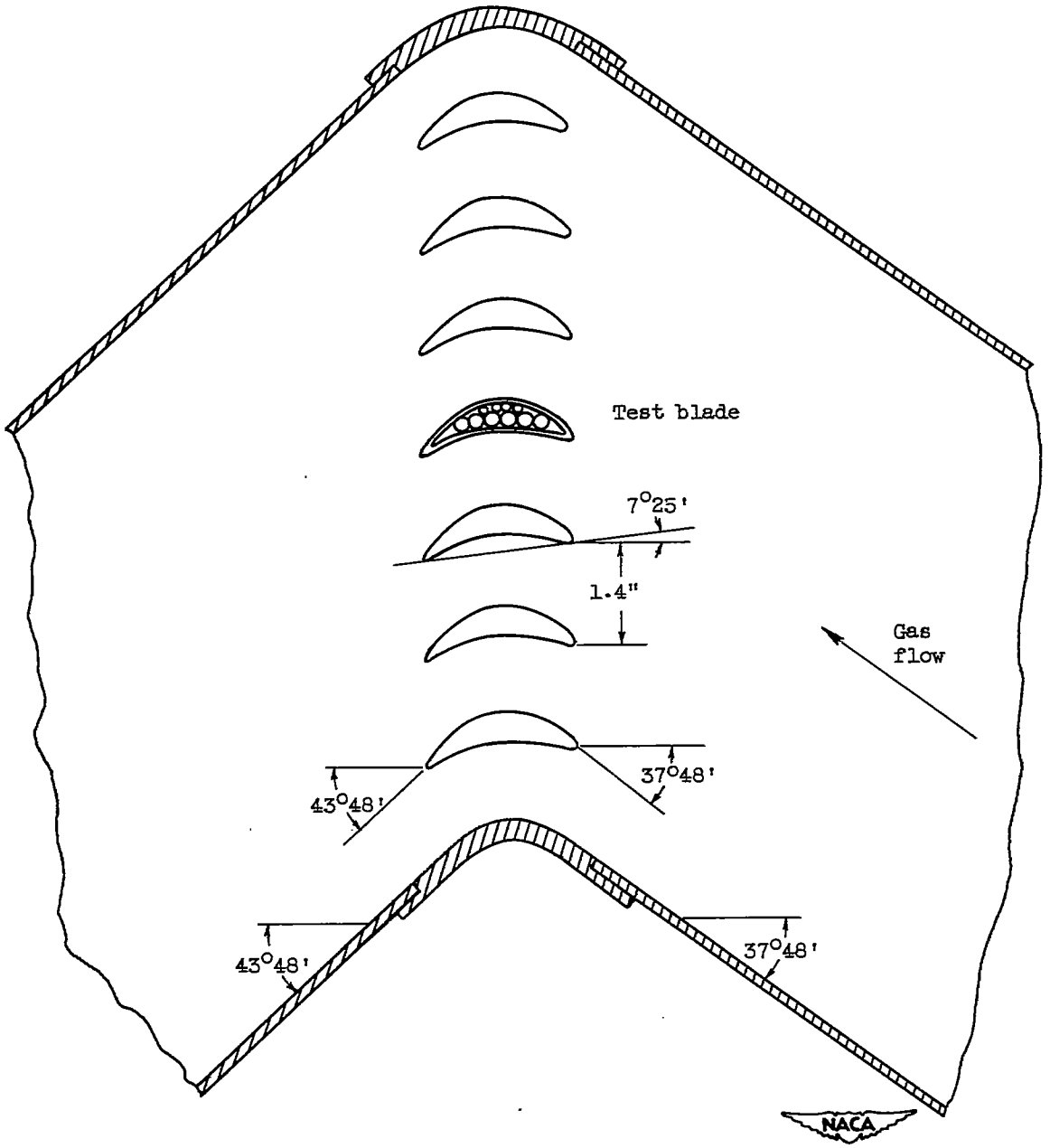

Figure 2. - Cascade geometry.

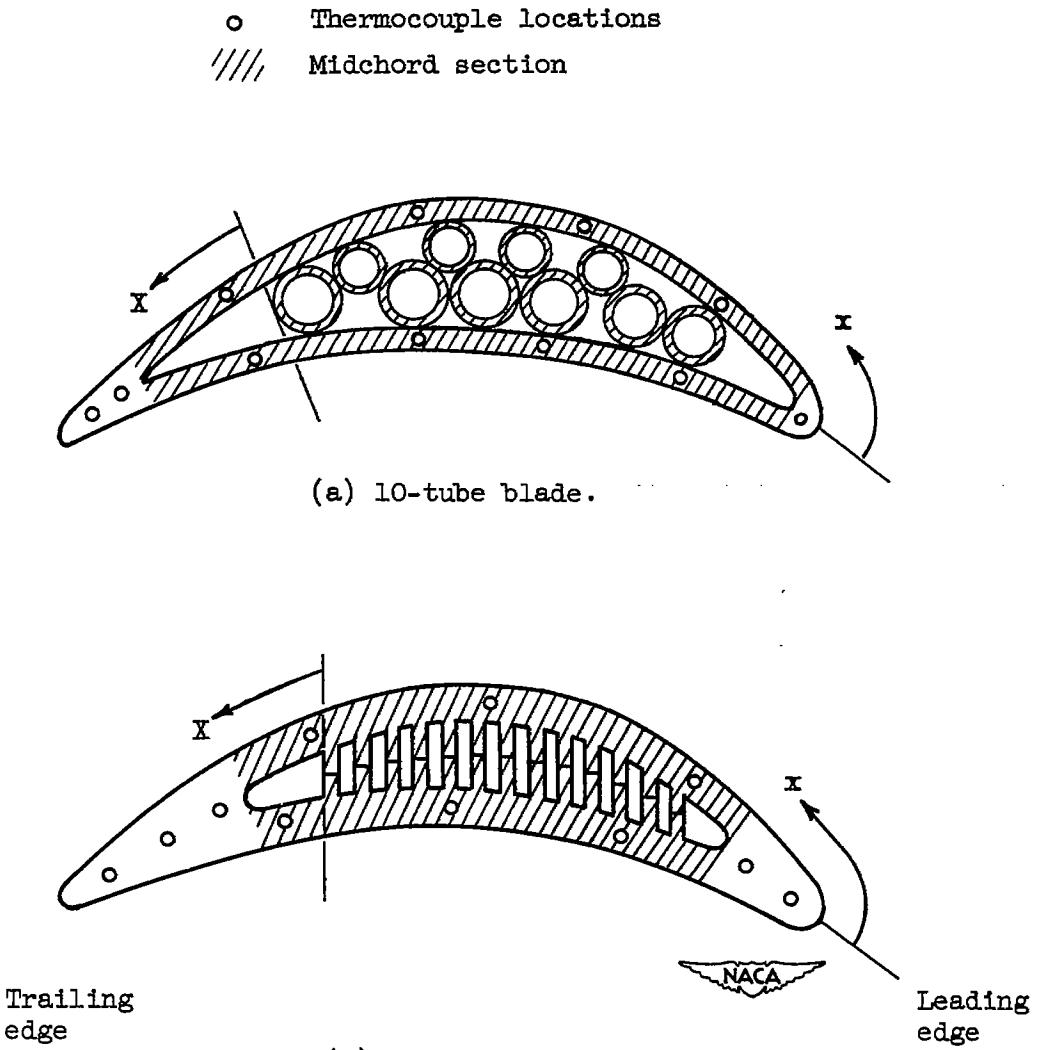

(a) 10-tube blade.

(b) 13-fin blade.

Figure 3. - Sectional view of test blades showing blade thermocouple locations.

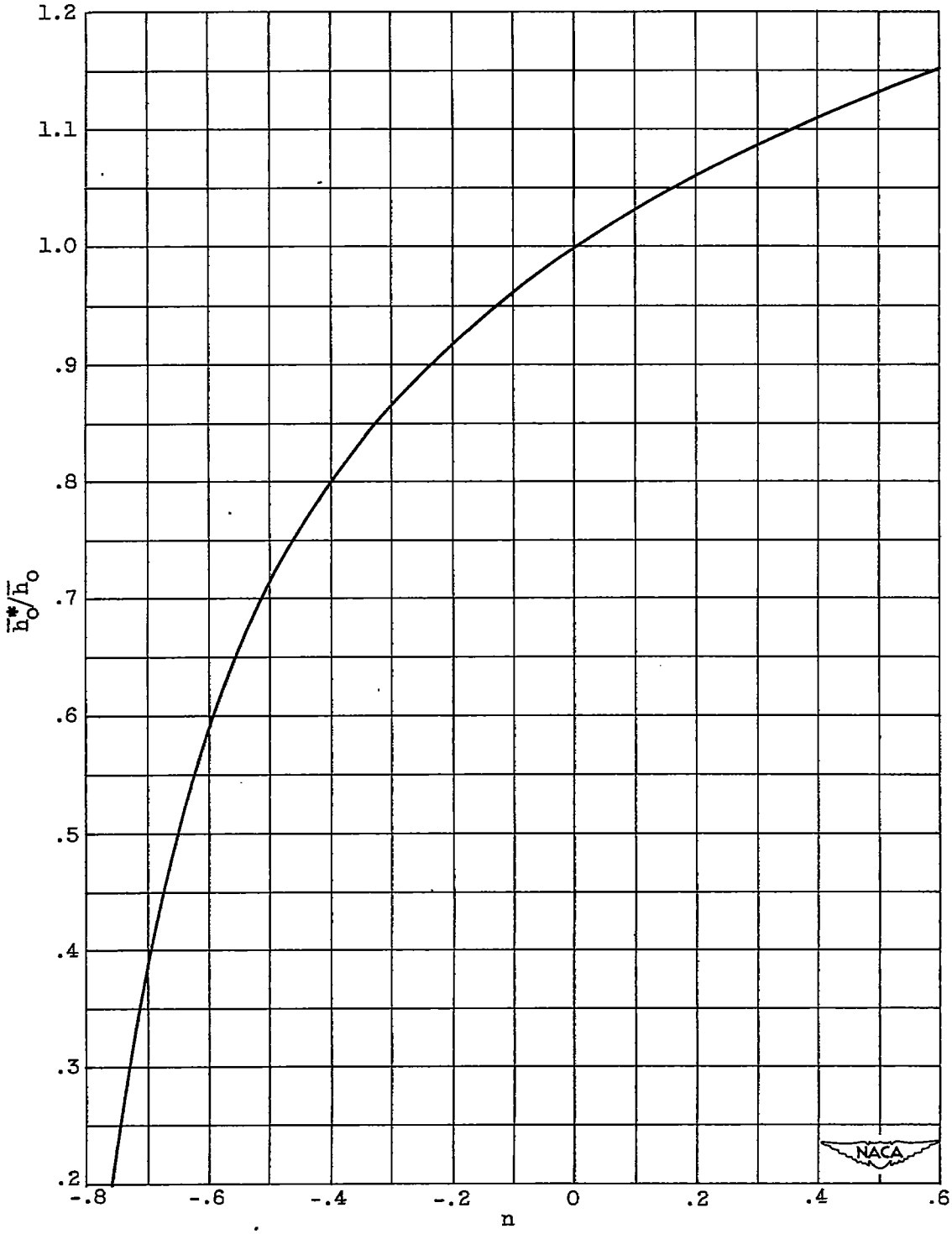

Figure 4. - Correction factor for gas-to-blade heat-transfer coefficients for variable wall temperature in turbulent boundary layer.

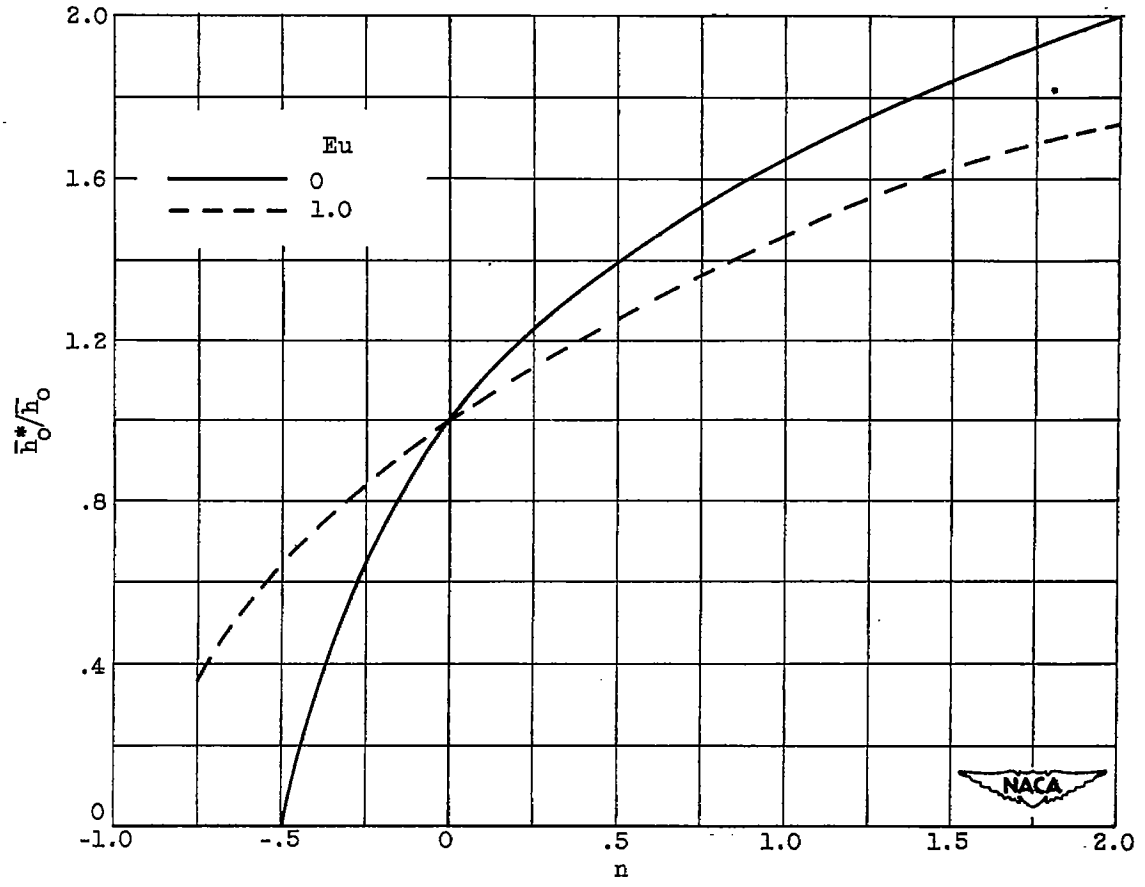

Figure 5. - Correction factor for gas-to-blade heat-transfer coefficients for variable wall temperature in laminar boundary layer.

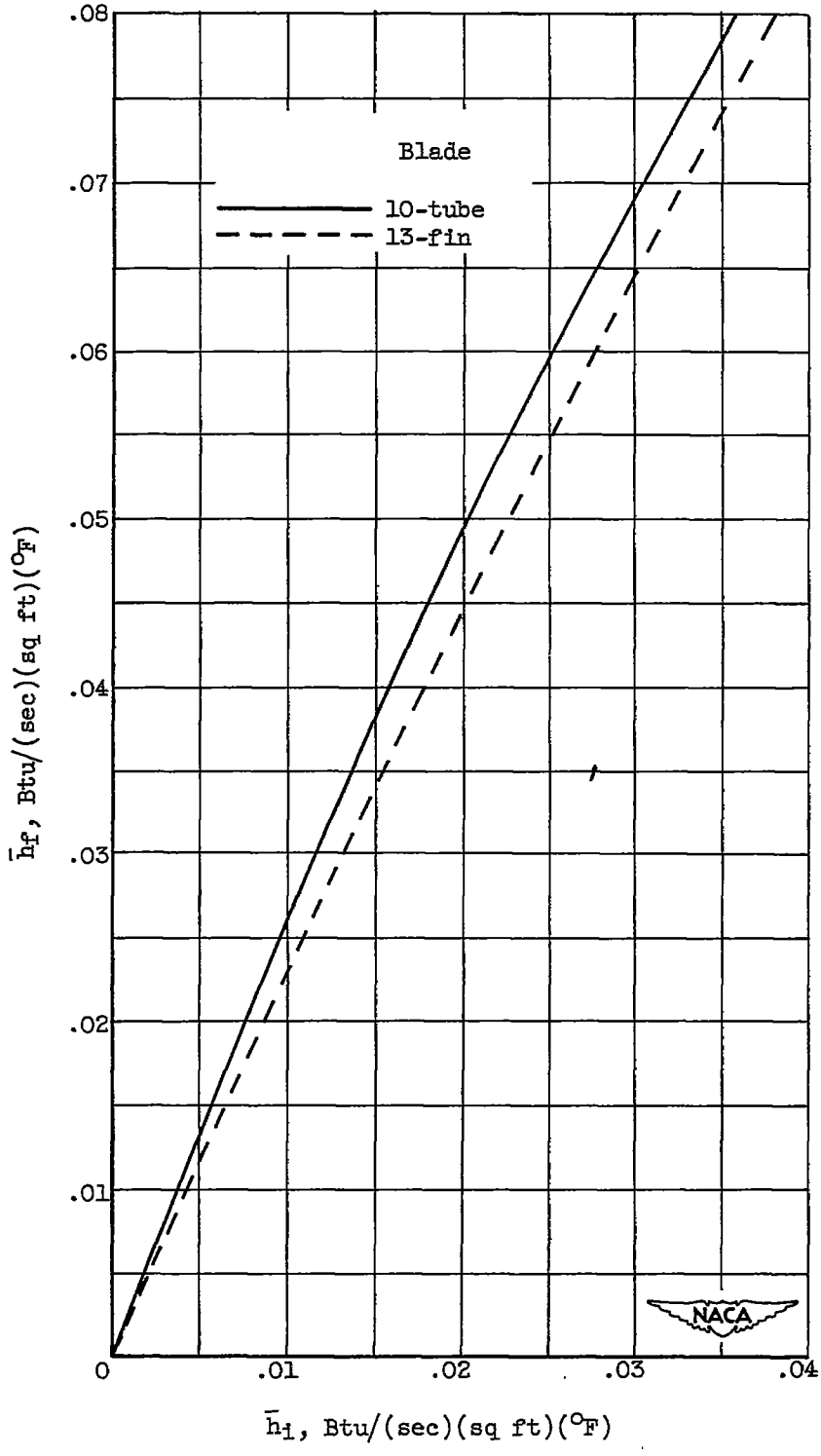

Figure 6. - Chart for determination of effective blade-to-coolant heat-transfer coefficients.

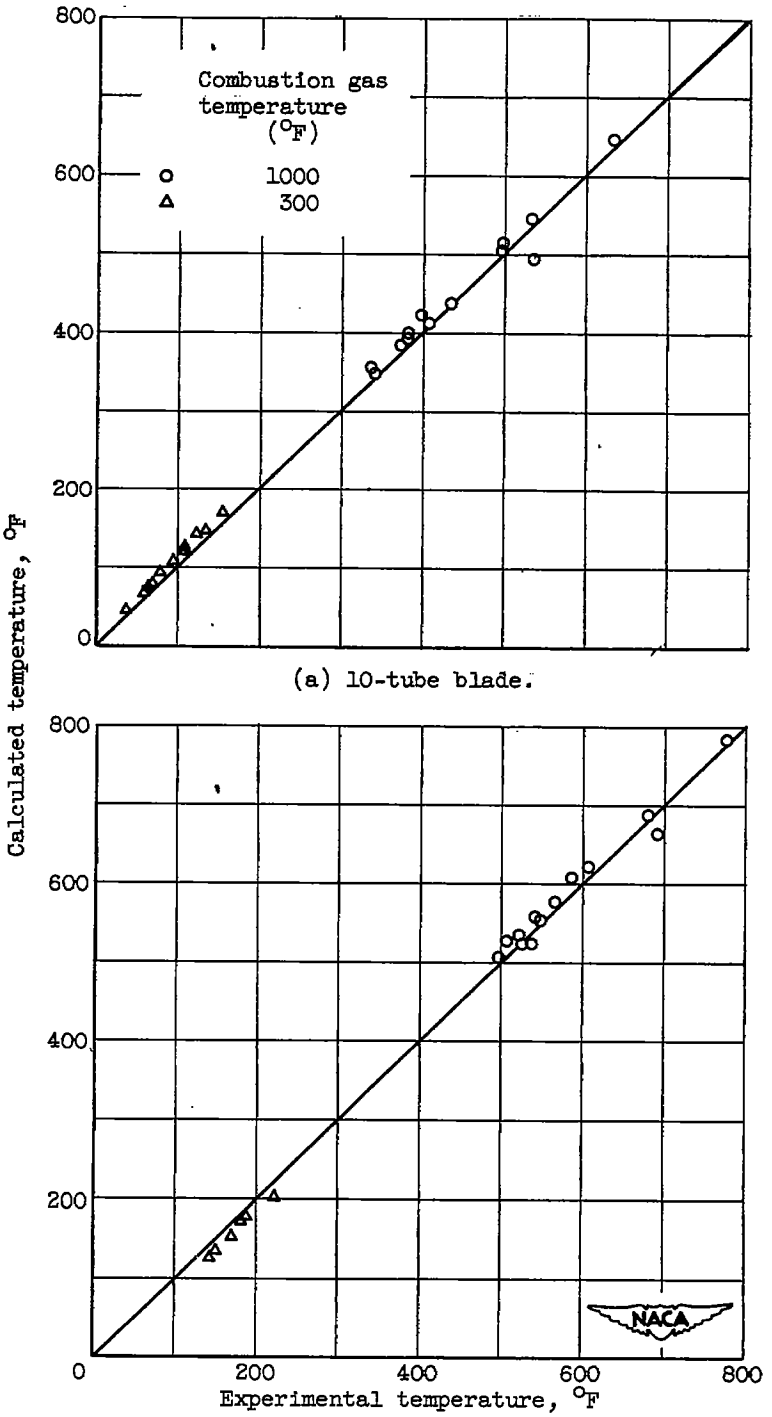

(a) 10-tube blade.

(b) 13-fin blade.

Figure 7. - Comparison of calculated average and experimental average midchord blade temperatures for two air-cooled blades in a static cascade.

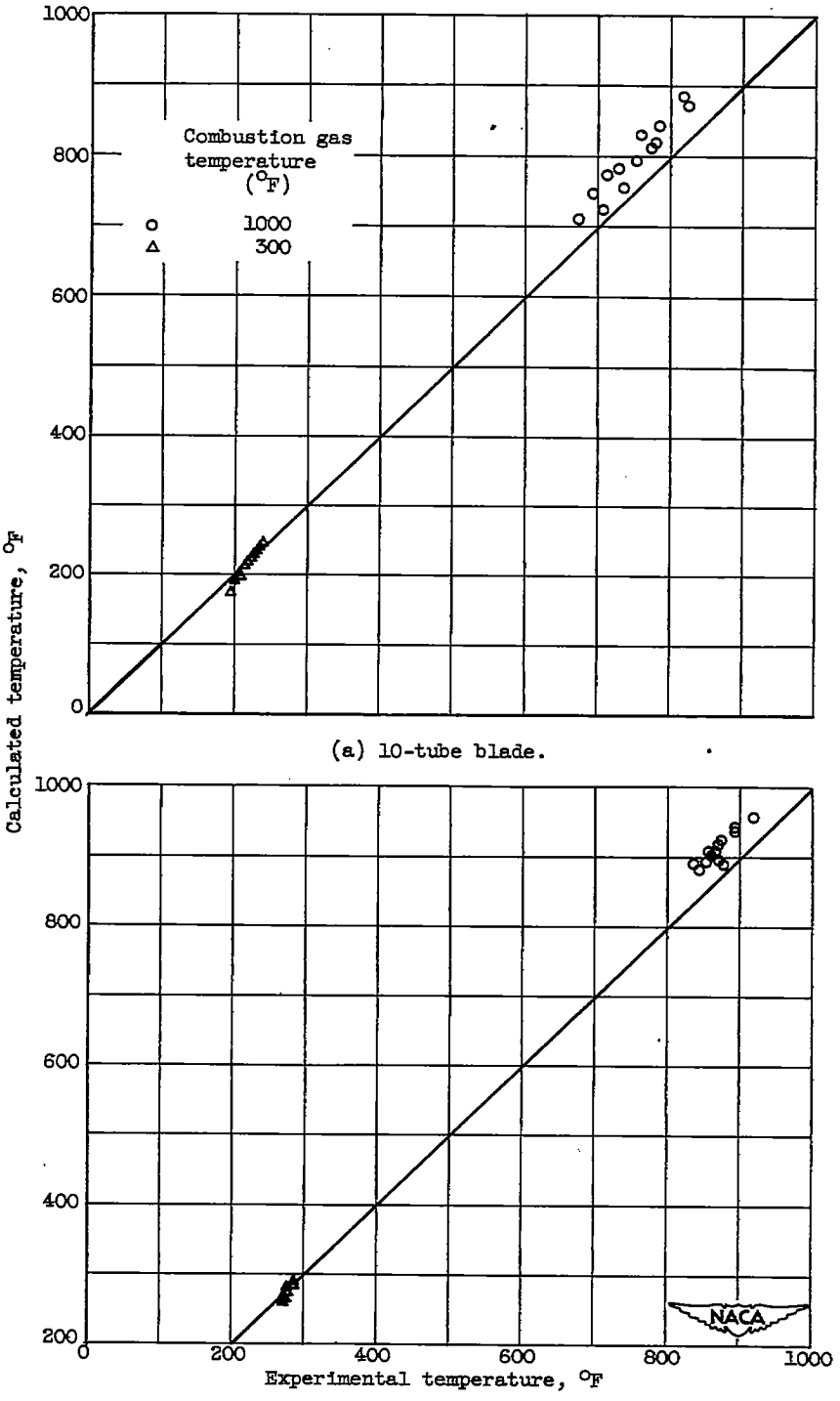

(a) 10-tube blade.

(b) 13-fin blade.

Figure 8. - Comparison of calculated and experimental local temperatures near blade trailing edge for two air-cooled blades in a static cascade.

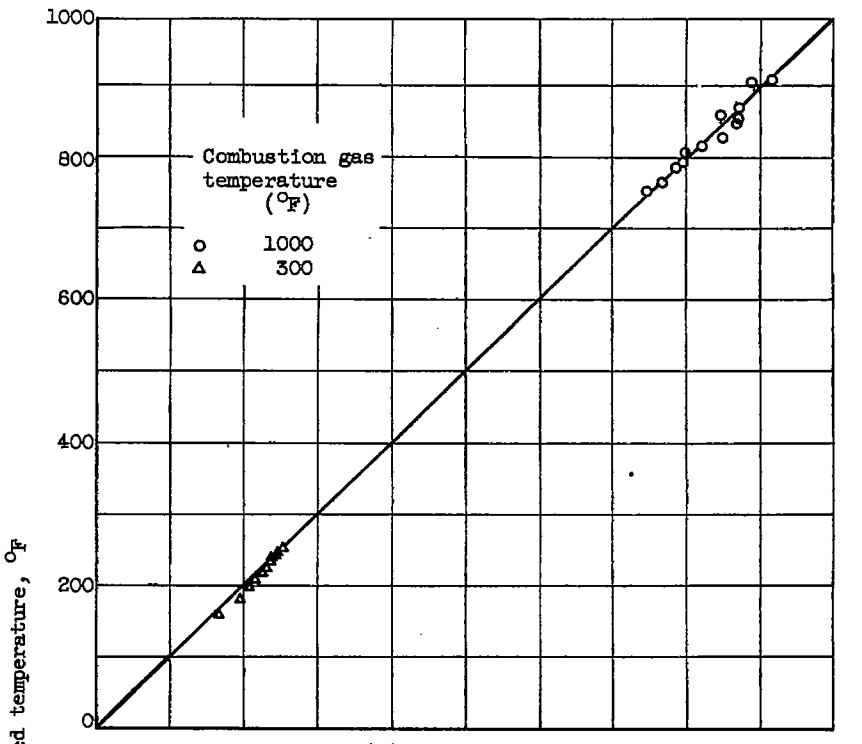

(a) 10-tube blade.

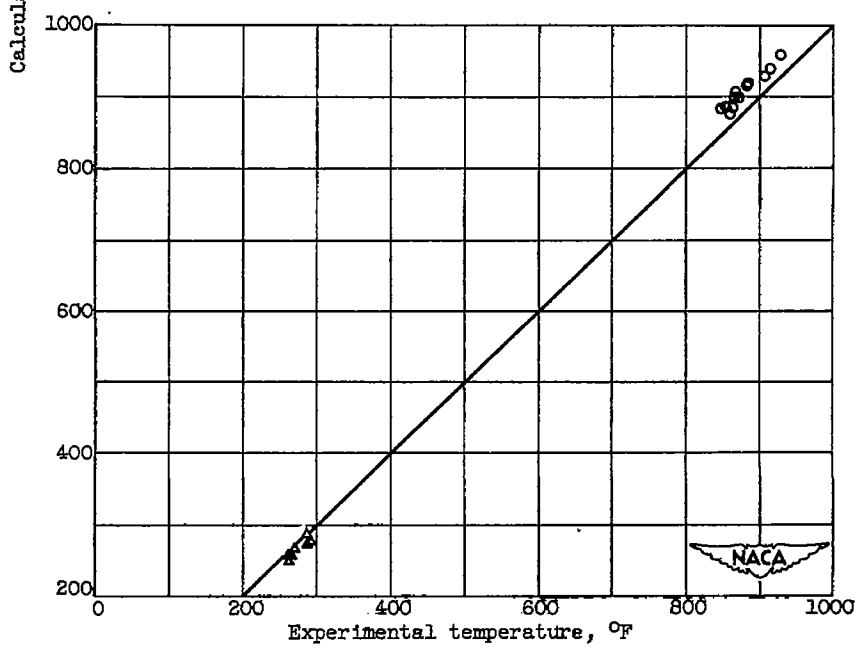

(b) 13-fin blade.

Figure 9. - Comparison of calculated and experimental local temperatures near blade leading edge for two air-cooled blades in a static cascade.

NACA-Langley - 9-29-52 - 400